# Lawrence Berkeley National Laboratory

**Title**
Assessment of ground-based monitoring techniques applied to landslide investigations

**Permalink**
https://escholarship.org/uc/item/2tw802pg

**Authors**
Uhlemann, S
Smith, A
Chambers, J
et al.

# Assessment of ground-based monitoring techniques applied to landslide investigations

Author links open overlay

panelS.UhlemannabA.SmithcJ.ChambersaN.DixoncT.DijkstraaE.HaslamaP.MeldrumaA.MerrittdD.GunnaJ.Mackaya

Show more

## Highlights

- High temporal resolution monitoring revealing rainfall triggered slope movements

- Investigation and comparison of long term landslide monitoring data sets

- Ground model development based on geotechnical/environmental data analysis

## Abstract

A landslide complex in the Whitby Mudstone Formation at Hollin Hill, North Yorkshire, UK is periodically re-activated in response to rainfall-induced pore-water pressure fluctuations. This paper compares long-term measurements (i.e., 2009–2014) obtained from a combination of monitoring techniques that have been employed together for the first time on an active landslide. The results highlight the relative performance of the different techniques, and can provide guidance for researchers and practitioners for selecting and installing appropriate monitoring techniques to assess unstable slopes. Particular attention is given to the spatial and temporal resolutions offered by the different approaches that include: Real Time Kinematic-GPS (RTK-GPS) monitoring of a ground surface marker array, conventional inclinometers, Shape Acceleration Arrays (SAA), tilt meters, active waveguides with Acoustic Emission (AE) monitoring, and piezometers. High spatial resolution information has allowed locating areas of stability and instability across a large slope. This has enabled identification of areas where further monitoring efforts should be focused. High temporal resolution information

allowed the capture of 'S'-shaped slope displacement-time behaviour (i.e. phases of slope acceleration, deceleration and stability) in response to elevations in pore-water pressures. This study shows that a well-balanced suite of monitoring techniques that provides high temporal and spatial resolutions on both measurement and slope scale is necessary to fully understand failure and movement mechanisms of slopes. In the case of the Hollin Hill landslide it enabled detailed interpretation of the geomorphological processes governing landslide activity. It highlights the benefit of regularly surveying a network of GPS markers to determine areas for installation of movement monitoring techniques that offer higher resolution both temporally and spatially. The small sensitivity of tilt meter measurements to translational movements limited the ability to record characteristic 'S'-shaped landslide movements at Hollin Hill, which were identified using SAA and AE measurements. This high sensitivity to landslide movements indicates the applicability of SAA and AE monitoring to be used in early warning systems, through detecting and quantifying accelerations of slope movement.

## 1. Introduction

Landslides form one of the major natural hazards causing loss of life and damaging of infrastructure worldwide. In the seven year period between 2004 and 2010, 2620 fatal, non-seismically triggered landslides were recorded worldwide, causing 32,322 fatalities (Petley, 2012). Although the landslide frequency in the UK is comparably low (e.g. some 754 reported events between 2006 and August 2015), the economic impact is high. Failure of engineered earthworks (embankments and cuttings) or adjacent natural slopes causes interruptions to transportation and utilities networks — a process that is affected by ongoing climate change and ageing of slope materials (Dijkstra and Dixon, 2010, Foster et al., 2011, Dijkstra et al., 2014, Glendinning et al., 2015, Pennington et al., 2015).

Since one of the primary triggering mechanism for landslides is intense or prolonged precipitation (Highland and Bobrowsky, 2008), the frequency and severity of landslides are expected to fluctuate with changes in precipitation patterns (spatial and temporal variations of duration and intensity). In a context of climate change, precipitation cannot be regarded as a steady state input and it is essential to develop robust models of adequate complexity that allow evaluation of possible future changes in slope instability due to forecasted changes in precipitation (Dijkstra and Dixon, 2010). Mid- to high-latitude regions are likely to face an increase in precipitation of up to 20%, including

increased flash floods due to more frequently appearing high-intensity rainfall events (Defra, 2012, Füssel et al., 2012). This increase in precipitation is likely to occur during the winter season, while summers will become drier (Defra, 2012). Wetter winters and drier summers will lead to an increased and deeper weathering of the topsoil, due to larger amplitudes in the wetting and drying cycles. This is likely to reduce the strength of the material and cause more frequent shallow slope instabilities. Understanding triggering mechanisms and failure potentials, to improve landslide forecasting, is therefore a major focus of research internationally.

Monitoring of kinematic, hydrological, and climatic parameters plays a significant role in supporting the development of slope stability models (e.g. Buchli et al., 2013, Springman et al., 2013), since without understanding movement patterns and responses to climate events, forecasting is not possible (Angeli et al., 2000). This requires not just monitoring of actual movements, but also environmental factors including rainfall, temperature, soil moisture content and relative (air) humidity, as well as geotechnical parameters, such as, pore water pressure. This enables the correlation of movement events with their triggering mechanisms and helps to inform the underlying causalities in the process–response models.

Previous studies have related deformation measurements by GPS/GNSS, inclinometer, extensometer or tilt meter readings to rainfall events (e.g. Malet et al., 2002, Corsini et al., 2005, García et al., 2010, Brückl et al., 2013) to study the deformation behaviour of rainfall triggered landslides. Additionally, Malet et al., 2002, Corsini et al., 2005, and Brückl et al. (2013) compare measurements of two or three of the mentioned conventional deformation monitoring techniques, showing good correlation between surface (e.g. GPS) and subsurface (e.g. inclinometer) deformations in terms of movement occurrences.

In this paper we introduce and compare conventional techniques, such as GPS, inclinometer and tilt meter, and recently emerging deformation monitoring techniques, such as acoustic emission (AE) monitoring using active waveguides (AEWG), and Shape Acceleration Array (SAA). To our knowledge, this is the first time that these monitoring techniques have been combined on an active landslide, providing long-term (2009–2014) measurements. This paper highlights the relative performance of these techniques focusing on different movement periods, and it provides detailed, integrated interpretations of movement, environmental, and geotechnical data of the Hollin Hill landslide. The paper reports how these long-term monitoring results have enabled a step-change in the understanding of slope dynamics, building upon previously published work.

The study site, where a Lias mudstone formation is failing, is typical for many inland landslides in lowland settings. Thus, the conclusions drawn from this study can provide guidance for researchers and practitioners for selecting and installing appropriate monitoring techniques to assess unstable slopes.

## 1.1. Slope monitoring instruments and techniques

There is a clear need to monitor landslides and marginally stable slopes to provide early warning of instability. This will allow for timely evacuation of vulnerable people, as well as timely repair and maintenance of critical infrastructure. The cost of remediation subsequent to landslide failure is several times higher than the cost of corrective measures and repairs if conducted prior to collapse (Glendinning et al., 2009); this highlights the importance of early warning through monitoring. Monitoring also provides: (1) the information necessary for slope stability analysis and remediation design, (2) knowledge of stability to and through construction, and subsequent to remediation, as well as (3) understanding of the condition (both serviceability and ultimate limit states) of adjacent infrastructure that has the potential to be impacted upon by slope instability (Dunnicliff, 1988, Machan and Beckstrand, 2012).

There are many different techniques and types of instrumentation typically used in slope monitoring, and numerous emerging technologies. No single technique or instrument can provide complete information about a landslide and therefore various combinations are usually employed. The primary parameters of interest are deformation and pore-water pressure. Information on these is necessary to assess the rate and magnitude of movement, as well as changes to effective stress and hence stability. Performance of monitoring techniques and instruments is usually assessed in terms of accuracy and precision, spatial and temporal resolutions, sensitivity, and reliability (Dixon et al., 2015). However, on most projects the predominant factor driving the choice of instrumentation and techniques is their cost. For this reason the majority of slope monitoring programmes comprise installation of inclinometer casings and standpipes, which are usually read at discrete and infrequent intervals of the order of months. Inclinometers allow the depth to any shear surface(s) to be identified and standpipes provide information on the ground water conditions; information that is necessary for stability assessment and remediation design. However, this mode of monitoring provides relatively low spatial and temporal resolutions, which is usually insufficient to provide early warning of instability.

Detailed in Table 1 are the monitoring instruments and techniques employed in this study, together with an indication of their spatial and temporal resolutions. The

resolution of the methods is a function of the nature of the installation and the extent of the sensor network. Note that the classification shown in Table 1specifically refers to the installation at the Hollin Hill study site. This combination of monitoring approaches was selected in order to: (1) provide relatively high spatial resolution of ground surface movements, (2) determine the depth to shear surfaces, (3) monitor subsurface deformation at localised areas with high temporal resolution, and (4) to monitor pore-water pressures at shear surface depths with high temporal resolution. This significant level of information provides the basis for a thorough assessment of each of the approaches in order to make recommendations for other landslide investigations.

Table 1. Monitoring devices installed at the Hollin Hill landslide field laboratory. For each system a brief description as well as an indication of its spatial and temporal resolutions is given. Spatial resolution is given on a local, i.e. measurement, and global, i.e. slope, scale.

| Instrument/technique | Description | Spatial resolution | | Temporal resolution |
|---|---|---|---|---|
| | | Local | Global | |
| **Surface deformation monitoring** | | | | |
| **Global positioning system (GPS)** | • Repeated survey of permanently installed markers using RTK/GNSS GPS with centimetric accuracy providing time-series of 3D topographical data. Allows for measurement of surface movements and deformations<br>• Permanent GNSS stations allow for high temporal resolution | Moderate | Moderate | Low |
| **Tilt meter** | • Installed near the ground surface providing an indication of landslide activity and an indirect measurement of deformation<br><br>• Most suitable for monitoring of landslides with a large rotational component of movement; translational movements are unlikely to be detected | High | Low | High |
| **Subsurface deformation monitoring** | | | | |
| **Conventional inclinometer** | • Installed in a borehole penetrating stable stratum below any shear surface (or potential shear surface). The annulus around the casing is backfilled with material having similar properties as the surrounding soil (e.g. bentonite-grout)<br><br>• A torpedo probe measures the inclination of the casing with depth, | High | Low | Low |

| Instrument/technique | Description | Spatial resolution | | Temporal resolution |
| --- | --- | --- | --- | --- |
| | | **Local** | **Global** | |
| | providing a horizontal deformation vs. depth profile | | | |
| | • Time-series data can be used to determine magnitude and rate of displacements, and depth to shear surfaces (Mikkelsen, 2003, Simeoni and Mongiovì, 2007, Wan and Standing, 2014)<br>• If an in-place probe or probe-string is installed and deformation is logged continuously then high temporal resolution can be acquired | | | |
| **Shape Acceleration Array (SAA)** | • Comprises a string of MEMS (micro-electrical–mechanical systems) sensors installed at regular intervals along the depth of a borehole, which penetrates any shear surface or potential shear surface<br><br>• Each sensor monitors displacement in x-, y- and z-directions with high accuracy and temporal resolution (Abdoun et al., 2012) | High | Low | High |
| **Active waveguide and Slope ALARMS sensor (i.e. AE monitoring)** | • Installed in a borehole penetrating any shear surface or potential shear surface. Comprises a steel waveguide (i.e. to transport AE signals generated at the shear surface to the ground surface with low attenuation) and granular backfill (i.e. to generate high energy AE as the slope deforms)<br><br>• AE is generated when the granular backfill is deformed by deformation of the host slope<br><br>• AE is measured at the ground surface with a Slope ALARMS system (Dixon and Spriggs, 2011)<br><br>• Recorded are AE rates or ring-down counts (RDC) per unit time, which are the number of times the signal amplitude crosses a pre-defined voltage threshold per pre-defined time period<br><br>• AE rates (e.g. RDC/h) are proportional to slope displacement rates, enabling detection of accelerations and decelerations of | High | Low | High |

| Instrument/technique | Description | Spatial resolution | | Temporal resolution |
| --- | --- | --- | --- | --- |
| | | Local | Global | |
| | slope movement (Dixon et al., 2003, Dixon et al., 2014, Dixon et al., 2015, Smith et al., 2014, Smith and Dixon, 2015) | | | |
| **Ground water monitoring** | | | | |
| **Piezometer** | • Piezometer tip is installed to depth(s) of interest (e.g. a shear surface) inside a borehole to monitor pore-water pressures of a certain depth range | Moderate | Low | Low to High |
| | • The annulus around the tip is backfilled with either sand or grout (dependent on the permeability characteristics of the host slope material) | | | |
| | • The remainder of the hole is backfilled with low permeability grout to form a closed/sealed system (Wan and Standing, 2014) | | | |
| | • Water levels in the piezometer can either be logged manually (low temporal resolution) or automatically (high temporal resolution) and can be used to calculate pore-water pressures within the screened interval of the piezometer tip | | | |

## 2. Study site

The landslide observatory is set on a south-facing hillslope, Hollin Hill, with a mean slope angle of 12°, located south of the village of Terrington, North Yorkshire, UK (54°06′38″ N, 0°57′30″W; Fig. 1). It is set in the Howardian Hills, an undulating landscape running approximately NW–SE shaped in four bedrock formations of Lower to Middle Jurassic age and covered by superficial deposits of variable thickness (Fig. 1b). Hollin Hill is a flat-topped hill capped by calcareous sandstone and ferruginous limestone belonging to the Dogger Formation (DF). There is a sharp boundary to the underlying Whitby Mudstone Formation (WMF), the failing formation at this site (Gunn et al., 2013). The WMF, showing a thickness of about 25 m (Chambers et al., 2011), is composed of grey to dark grey mudstone and siltstone with scattered bands of calcareous and sideritic concretions (Chambers et al., 2011). It overlies the Staithes Sandstone Formation (SSF). The boundary between these two formations is

represented by an upward transition from sandstone or siltstone to shaley mudstone. This change in depositional facies is marginally episodic and, although a fining upward trend persists, the boundary between the SSF and WMF is manifested by sequences of ferruginous, micaceous siltstone, with fine-grained sandstone and thin mudstone partings. The SSF is heavily bioturbated and shows local occurrences of siderite and pyrite (Gaunt et al., 1980). The formation underlying the SSF is the Redcar Mudstone Formation (RMF) that comprises grey, silty, calcareous, and sideritic mudstone with thin shelly limestones (Powell, 1984, Powell, 2010). The DF represents a potential aquifer above the WMF. Hydrogeological characterisation of the WMF and SSF is very complex as a result of variations in particle size in sedimentary sequences that, in turn, may be disturbed by bioturbation and inter-connected joint systems.
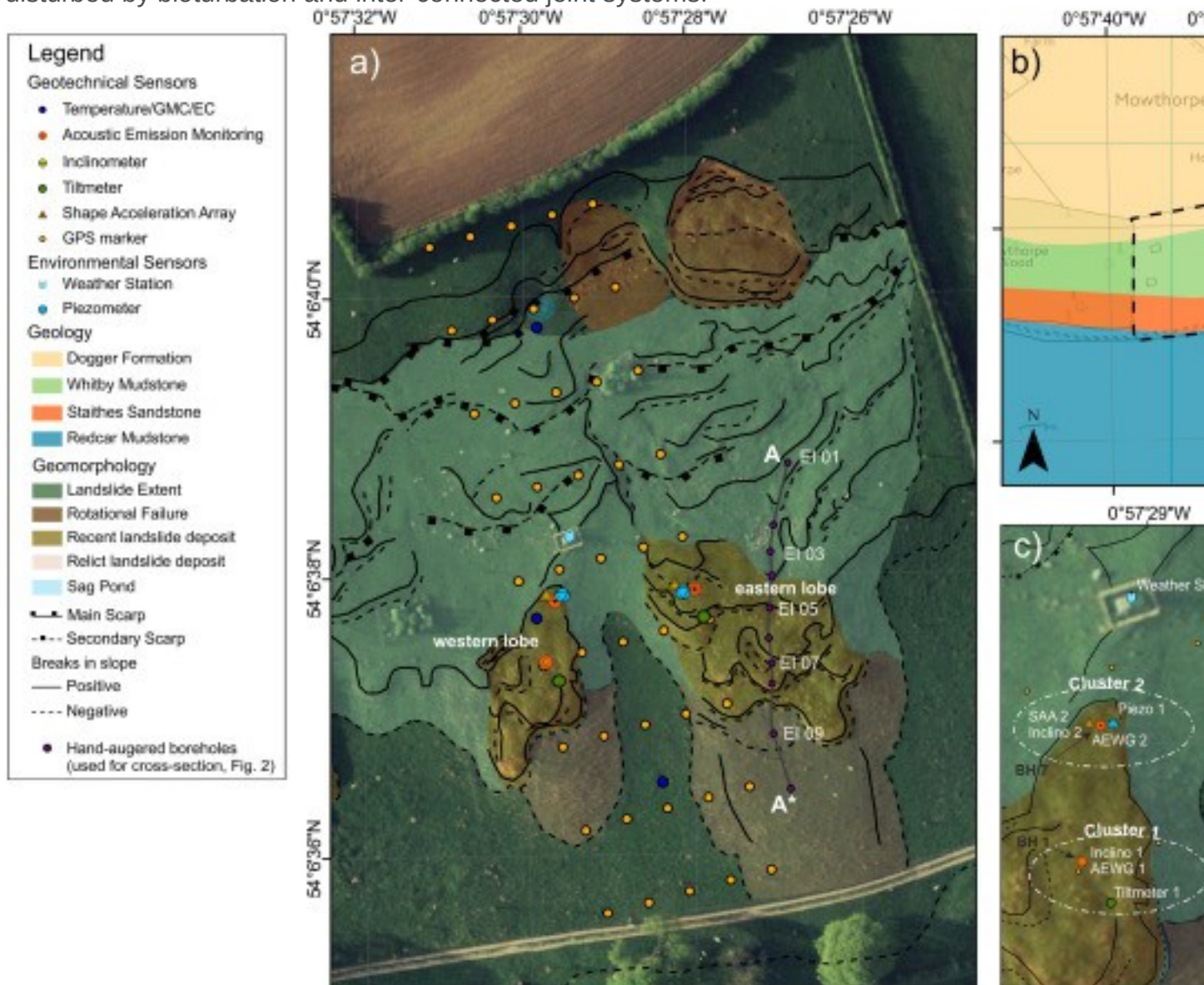
Fig. 1. Overview maps of the study site. a) Geomorphological map of the landslide indicating different landslide bodies and features (after Merritt et al., 2013). Also shown are the locations of the monitoring equipment that are deployed at the site and discussed in this paper. b) Geological setting of the study site; inlet shows location within the UK. c) A section of Fig. 1a at a larger scale showing the locations of sensor clusters comprising inclinometer, AEWG, SAA, piezometer, and tiltmeter deployed on the two lobes, as well as the location of the weather station. Note that cluster 1 comprised AEWG logging during February 2010 to December 2010; the locations of the SAAs at clusters 2 and 3 are adjacent to the locations of inclinometers 2 and 3.

On top of much of the lower slopes in the SSF, a thin (up to 2 m thick) fine sand deposit is found, preserving the old slope and head deposits. It is likely that this sequence represents a periglacial slope with associated coversand (e.g. Catt, 1977, Ballantyne and Harris, 1994, Bateman, 1995). The persistence of a thin head deposit on top of the SSF suggests that the old (periglacial) slope profile has been largely preserved by the subsequent cover of the aeolian sands.

The Hollin Hill landslide is in many ways representative of inland landslides in stiff clays and is acting as a field laboratory to provide, amongst others, a test site for a range of monitoring techniques, including the ALARMS (e.g., Dixon et al., 2010, Dixon et al., 2014, Smith et al., 2014) and ALERT systems (e.g. Kuras et al., 2009). So far, the geological and geomorphological characterisation was mainly informed by geophysical data, borehole logs and inclinometer readings during periods of very-slow movement (~ 0.5 m year$^{-1}$; Chambers et al., 2011, Merritt et al., 2013). This paper utilises previously unavailable data to focus on periods of landslide reactivation with movements of up to 3.5 m year$^{-1}$, leading to a better informed interpretation of landslide processes and characterisation of the site.

Merritt et al. (2013) provide a preliminary geomorphological characterisation of the slope together with an initial assessment of a ground model. An updated and more detailed ground model is presented here based on the interpretation of borehole and geotechnical data. Characterisation of the morphogenesis of this slope is supported by a section constructed on the basis of a series of shallow (up to 4 m depth), hand-augered boreholes (Fig. 2).
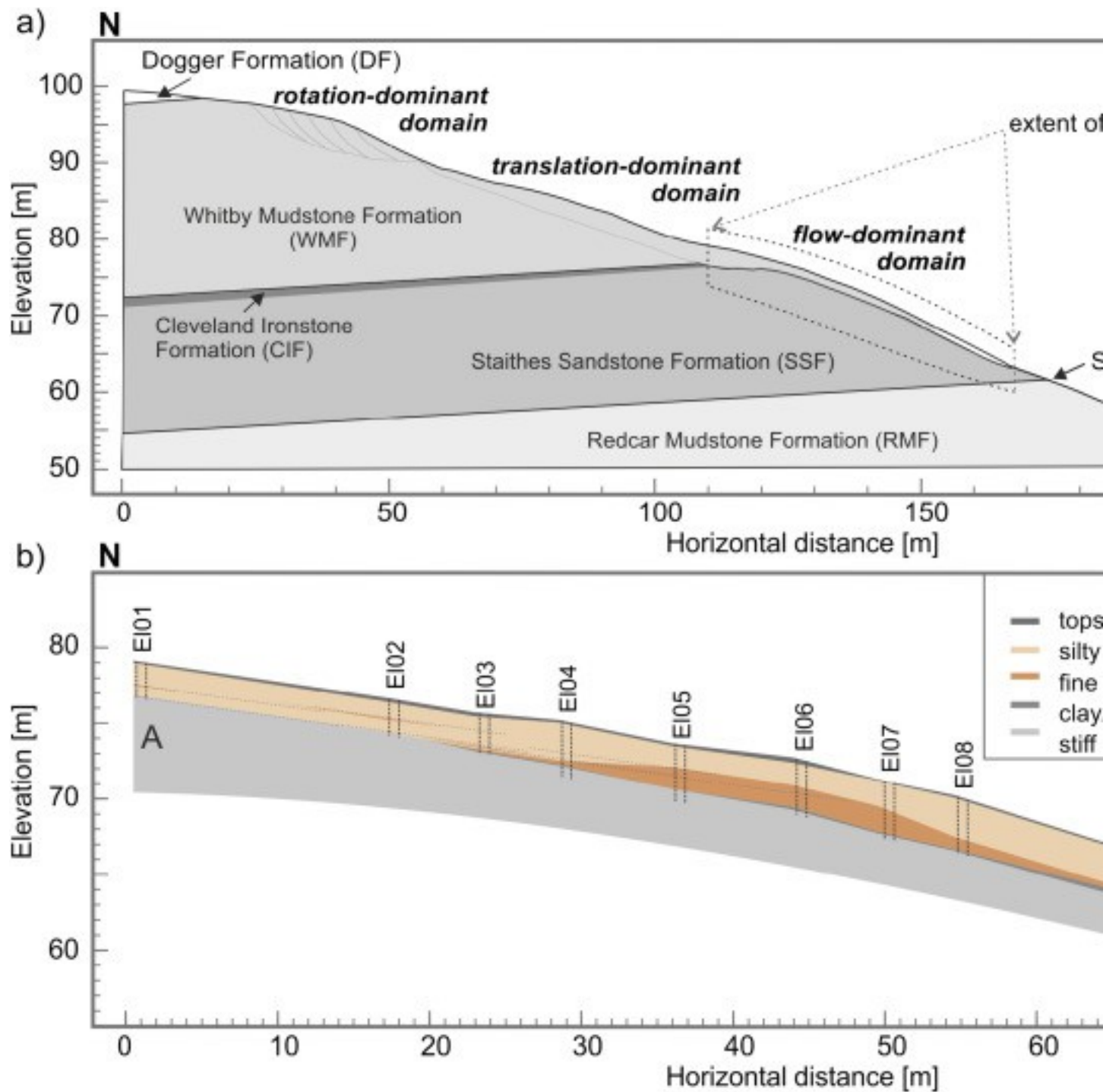
Fig. 2. Representative section of the stratigraphy and slope instability domains for Hollin Hill. a) Diagram modified after Gunn et al. (2013). b) Profile A–A* through the eastern lobe informed by hand augered holes down to depth of 4 m (profile location indicated in Fig. 1).

In summary, Hollin Hill comprises a largely linear slope that is affected by different types of slope instability that can be sub-divided into three domains (with fuzzy boundaries; Fig. 2).

- In the central section translational landsliding in the WMF dominates. Multiple translational components can be distinguished and discrete shear zones have been observed in boreholes in this central part of the slope complex.

  - With progressive displacement of the translational slides, disintegration of the slide mass occurs, leading to slope deformation that is increasingly characteristic of flow-like behaviour further down the slope.

    - The slopes above the central section display recent, rotational deformation. Progressive translational deformation in the central domain leads to unloading and oversteepening of the toe of the upper slopes, resulting in landsliding that is dominated by sliding along curved slip surfaces.

Note that the instrumentation clusters described in this study are installed in the translation/flow-dominant zone. The translation/flow-dominant lobes located in this zone are simply referred to as lobes hereafter.

Instability in the WMF involved sequences of thin translational slide or flow events. Multiple slip surfaces and stretched out, thin bands of aeolian sands provide some evidence that phases of deformation have occurred subsequent to the aeolian deposition.

The steepest slope angles are found where the slope is developed in the SSF. As the translational-flow slide deformation in the WMF reaches this steeper section, it would be logical to expect the development of further runout, but instead a series of ridges are observed. Progressive deformation of the translational-flow slides appears to be impeded by base draining as the landslide moves over the fine sands further down the slope.

A substantial thickness of fine sand is found between boreholes El04 and El08 (hand-augered boreholes, Fig. 2). This local accumulation may reflect uneven aeolian deposition, but it is also plausible that landslide activity in the WMF incorporated some

sand in the slope deformation process, driving this surface veneer onto the sand further down the slope and thus creating a local accumulation. This latter scenario is supported by the inclinometer data of Fig. 3. It shows borehole logs and the results of cumulative inclinometer measurements conducted over a period of 2.5 to 3 years. It is evident that the lowest active shear surfaces occur in the fine sandy deposits at a depth of approximately 1.5 m at the western lobe (BH 1 and 7). The profiles also suggest the existence of further slip surfaces or flow-like deformation in more shallow deposits.
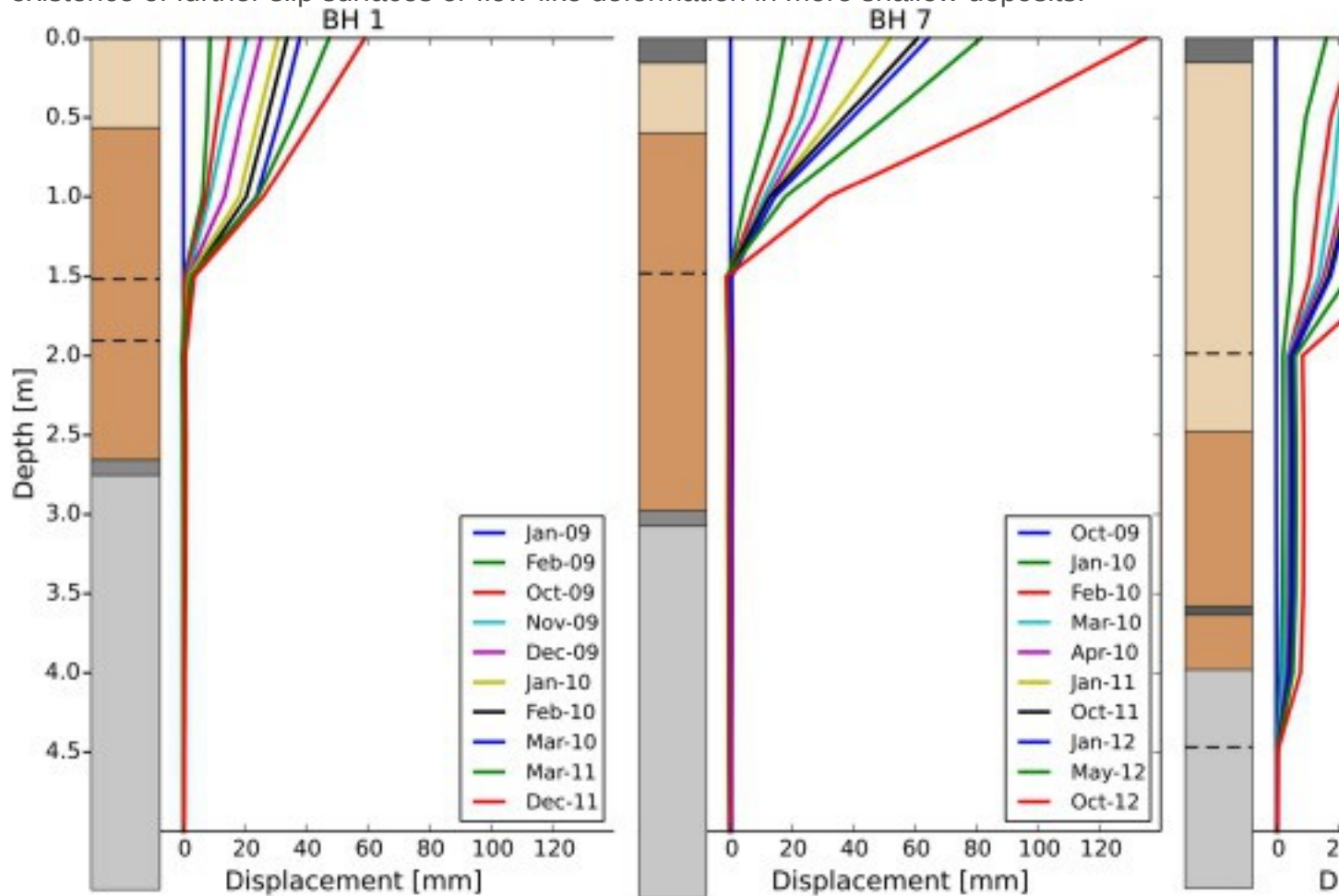
Fig. 3. Borehole logs and corresponding inclinometer data highlighting slip surfaces. Boreholes 1 and 7 (BH1 and BH7) are located on the western lobe (Inclinometer 1 and adjacent to SAA2 in Fig. 1c), Borehole 5 (BH5) on the eastern lobe (adjacent to AEWG 3 in Fig. 1c).

The profile representing the eastern lobe (BH 5) is more complex. This borehole is set in an accumulation ridge where ongoing deformation in the upper WMF is inhibited by toe

draining through the underlying fine sands. This is clearly illustrated by the relatively thick silty clays overlying the fine sands. In these silty clay landside deposits shear surfaces are observed at about 2.0 m depth, i.e. about 0.5 m above the boundary with the fine sands, and these observations are supported by the inclinometer data. At approximately 4 m depth there appears to be a second shear surface resulting in very slight deformation of up to 10 mm over a period of 3 years.

The aeolian sands within and below the landslide deposits have a complex relationship with the deformation behaviour of this slope. When incorporated in the slide body, it is possible that these sand lenses act as interceptors for diffuse inflow of water, and are potentially capable of generating artesian pore pressures at critical depths.

## 3. Instrumentation installation

As already mentioned and shown, this landslide is equipped with a range of monitoring systems to serve as a research landslide observatory to improve our understanding of triggering mechanisms for first time failure and landslide reactivation. The following monitoring systems are deployed on the slope and were actively monitoring as indicated:

- 
  Three clusters of active waveguides monitoring acoustic emission (2009–ongoing)

  - 
  Three inclinometers (2008–2012)

    - 
  Two shape acceleration arrays (2013–ongoing)

    - 
  Two tilt meters (2008–ongoing)

      - 
  GPS tracking of 45 marker points (2008–ongoing)

      - 
  Weather station (2008–ongoing)

- Two piezometers (2009–ongoing)

Additionally, soil moisture content, bulk conductivity and temperature are monitored at three different locations, covering the backscarp, active lobes, and an area outside of the landslide, with sensors deployed at different depths below ground level (bgl) ranging from 0.1 to 6.5 m. The location of the different monitoring systems can be found in Fig. 1a, c. This range of different monitoring systems, each characterized by different accuracy, sensitivity, and spatial and temporal resolutions provides the basis for a thorough assessment of techniques used for slope monitoring.

In the following a brief description is provided for each monitoring system.

## 3.1. Active waveguides (AEWG)

The active waveguides were installed in 130 mm diameter boreholes to depths of 5.7 m bgl; each comprises 6 m long, hollow steel tubing of 50 mm diameter and 3 mm thickness. The annulus around the steel tubing was backfilled with angular 5 to 10 mm gravel compacted in nominally 0.25 m high lifts. The top 0.3 m of the boreholes were backfilled with a bentonite grout plug to seal against the ingress of surface water (Fig. 4). The gravel backfill, which is acoustically noisy, generates high-amplitude AE signals. This overcomes the limitation of detecting low-amplitude AE signals caused by slope movement of the fine-grained, acoustically quiet, host material (Dixon et al., 2003). Transducers were coupled to each of the waveguides at the ground surface and were connected to Slope ALARMS (Dixon and Spriggs, 2011) sensors which were powered by batteries and recharged by solar panels; logging was at 30-min intervals. These AE monitoring systems, which inform only about the behaviour of the installation borehole, provide globally a low spatial resolution, but deliver information on rates of subsurface deformation (i.e. accelerations and decelerations) with high temporal resolution.
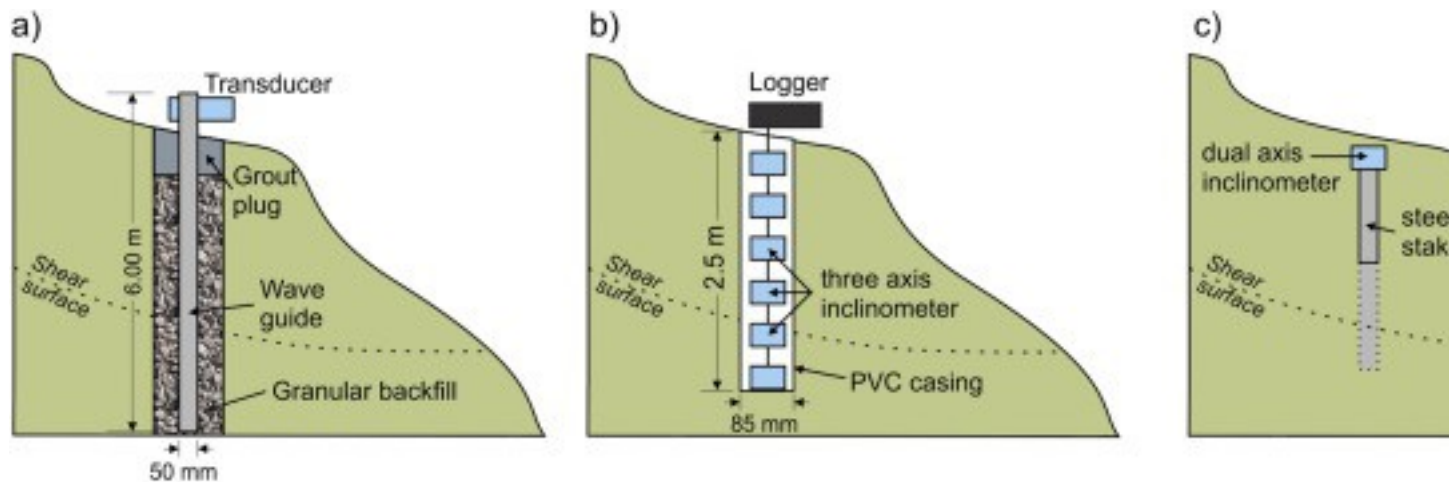
Fig. 4. Schematic illustration of permanently installed subsurface movement monitoring techniques; a) AEWG monitoring, b) SAA, and c) tilt meter. Note, employing a longer stake for the tilt meter and fixing it below the shear surface (dashed installation) will induce a larger proportion of rotational movement..

### 3.2. Inclinometers

Inclinometer casings were installed at the three cluster locations and approximately 1 m east from the active waveguides with keyways orientated along the slope dip- and strike-directions. The inclinometers penetrated to depths of 6 to 7 m bgl. They ceased to be usable after 3 years of monitoring in November 2012 due to significant shear surface displacement inducing localised bends within the casing sufficient to no longer allow the torpedo probe to pass.

Inclinometers provide relatively low global spatial resolution as a survey of the casing only informs of deformation in the soil surrounding the borehole. If casings are surveyed manually using a torpedo probe, relatively low temporal resolution with intervals of the order of months can be obtained (NB — higher temporal resolutions can be achieved by using in-place probes).

### 3.3. Shape Acceleration Array (SAA)

SAAs were installed approximately 1 m west of AEWG2 in May 2013 and AEWG3 in December 2013 to provide continuous subsurface deformation measurements; their installation was instigated subsequent to the inclinometer casings no longer being usable. They were installed to depths of 2.5 m bgl. Each of the MEMS sensors that comprise the SAA log deformation at 1-hour intervals. The SAA operates in a similar

manner to an in-place inclinometer in that it provides deformation vs. depth measurements with high temporal resolution ([Fig. 4](#)).

## 3.4. Tilt meter

Tilt meters were installed to monitor small changes in surface inclination, related to rotational downslope movement of mass that is evident at several trees on site. Each tilt meter consists of a dual axis inclinometer sensor with an accuracy of 0.1° mounted on a 0.5 m long coated iron stake ([Fig. 4](#)). The two tilt meters were connected to a data logger recording tilt angles hourly.

Tilt meters provide point measurements only that are representative for a small area within the landslide (and thus low global spatial resolution) and monitor tilt as opposed to actual deformation; however, they log data with high temporal resolution enabling correlation of movement with rainfall-induced instability.

## 3.5. Tracking of GPS markers

GPS markers were distributed regularly as five parallel lines of nine markers each, and made of wooden pegs. Inline marker separation was about 20 m, while line spacing was about 10 m. Their initial positions were surveyed using a real-time kinematic GPS equipment, providing centimetric accuracy. Every 1–2 months these markers were re-surveyed using the same equipment, building a time-series of landslide movements at those locations.

This approach provides a moderate spatial resolution, both, on local (i.e. marker) and global (i.e. slope) scales. It allows for identification and mapping of areas of activity across the slope, forming the basis for deciding where more sensitive instrumentation is to be installed (NB — depending on the available resources fine grids and permanent GNSS logging stations can be employed, delivering high spatial and temporal resolutions).

## 3.6. Weather station

The weather station was an all-in-one system measuring barometric pressure, humidity, precipitation, temperature, and wind speed and direction, with an hourly frequency. To minimize the effects upon the system from vegetation and other installations at the site, especially on the measurement of wind speed and direction, the weather station was placed on top of a pole at a height of 3 m. The data were recorded and stored using the same data logger as for recording the tilt meter readings.

### 3.7. Piezometers

Piezometers were installed in boreholes hand augered to 2.85 and 2.8 m on the western and eastern lobes, respectively. These depths were chosen in order to place the active zone of the piezometers in the vicinity of the depth to predicted shear surfaces, which were determined using CPT measurements (Gunn et al., 2013). We installed a 19 mm uPVC pipe, fitted with a 0.9 m slotted, porous piezometer tip in the borehole. The hole was backfilled with clean sand to 1.95 and 1.75 m below ground for the western and eastern piezometers, respectively, forming an active zone that allows for monitoring of the pore water pressure in the region of the slip surface located at about 1.6 and 1.9 m depth, respectively. The remainder was backfilled using bentonite granules to ensure sealing. The piezometric head measured in these standpipes is referred to the top level of the sand pocket forming the active zone, thus positive heads present conditions of positive pore water pressure. Since the active zones of the piezometers are in close proximity to the shear surface (< 0.35 m), the measured pore water pressures are indicative for the conditions at the shear surface. The water levels in these piezometers were logged with a 30 min interval. Note that the eastern piezometer experienced severe bending and became unusable in January 2013. It was reinstalled in December 2013, although slightly deeper (now 0.5 m below the shear surface).

It is important to highlight that the monitoring clusters are distributed over the two lobes, rather than installed adjacent to each other. Thus, times of activation may vary depending on their location on the lobe.

## 4. Interpretation of slope deformation

### 4.1. Delineation of regions of slope instability

Table 1 shows that the different monitoring techniques deployed have different spatial and temporal resolutions. To indicate their ability to differentiate movements at the system and over a typical slope scale, their spatial resolution has to be divided into two scales, local and global. While the tilt meter, AEWG, and SAA are sensitive to very small movements and thus have high local spatial resolution, their global spatial resolution is rather poor, since their recordings are determined by movements in their vicinity only. However, they can record movements with a high temporal resolution, allowing for a correlation of movement events with climatic circumstances, such as specific rainfall events. GPS marker and inclinometer measurements on the other hand have low temporal resolution, but can easily be used to determine areas of instability (GPS

markers) and shear surfaces (inclinometer) on a slope scale. Fig. 5 highlights this ability of GPS marker measurements to determine regions of slope instability and active movements. These measurements can be used to (1) show the direction and amplitude of surface deformations at monitoring points (Fig. 5a) and (2) to provide a map of the 5-year average landslide movement rates covering the entire slope (Fig. 5b) by interpolation of the monitoring points (Uhlemann et al., 2015). Between 2009 and 2014 the lobes experience significant surface deformations, with the eastern lobe showing significantly higher activity than the western, while the remaining areas show little or no deformation.
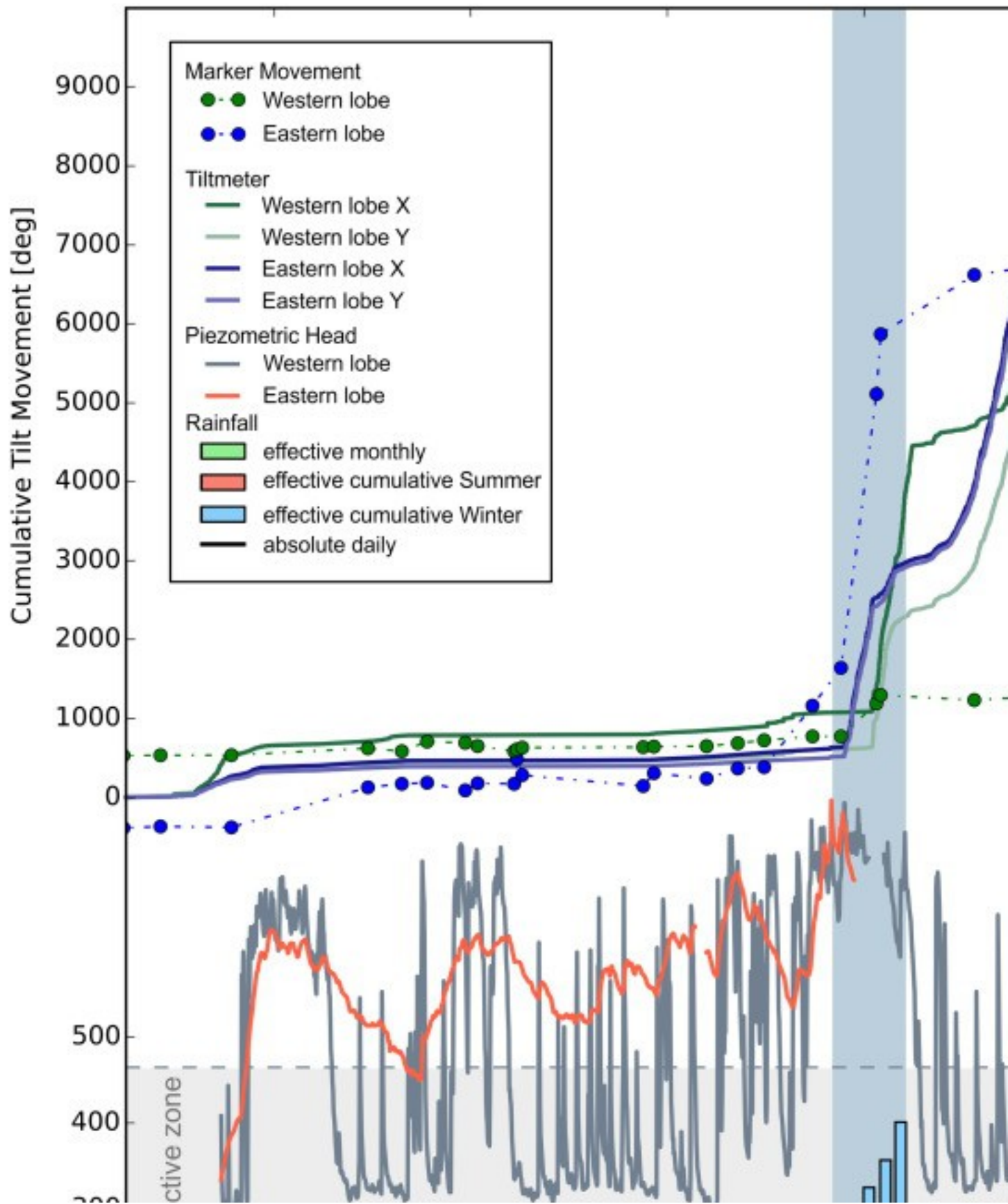


1. Download high-res image (1MB)

2.
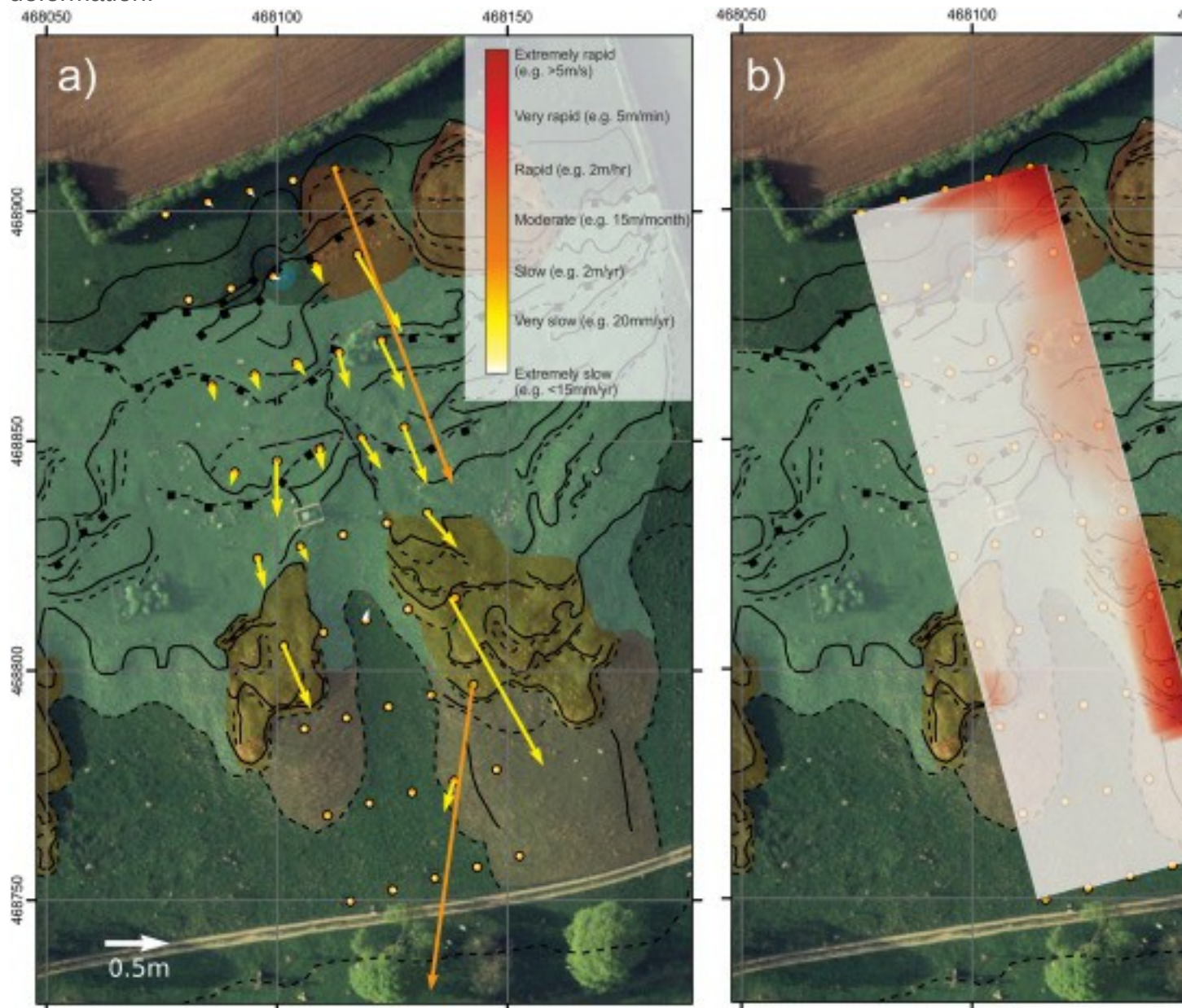
Fig. 5. Displacements determined from GPS marker surveys between 2009 and 2014 superimposed on the geomorphological map after Merritt et al. (2013). a) Displacement vectors (i.e. direction and amplitude); arrows show absolute surface deformation over the 5-year monitoring period. The colour of the arrows corresponds to the standard classification for landslide movement rates after Cruden and Varnes (1996). b) Map of average landslide movement rate (after Uhlemann et al., 2015) highlighting the activity of the eastern lobe and the connection between rotational failure of the backscarp and translational movements of the lobe.

Fig. 5 shows that the rotational movements in the backscarp are directly connected with translational movements of the lobes. Such investigation is only possible with a distributed network of deformation measurements offering reasonable spatial resolution on both scales. Hence, studies of movement patterns are only possible either with distributed subsurface monitoring devices or limited to surface deformation monitoring. In its current application the data suffer from low temporal resolution due to the need to survey positions manually. Therefore, the timings of periods of activity can only be approximately determined. The approach introduced by Buchli et al. (2012)would overcome this limitation by employing wireless GPS sensor networks that could log deformations nearly continuously. Recent studies on tracking electrode movements by employing electrical resistivity monitoring data (Wilkinson et al., 2010, Wilkinson et al., 2015) introduce another technique to obtain surface movement information on a global scale with high temporal and spatial resolutions.

4.2. Characteristics of the 5-year monitoring period

Fig. 6 shows rainfall, water level, cumulative tilt, and GPS marker movements for the monitoring period from the beginning of 2009 to 2014 (five years). Note that the GPS movement data shown in Fig. 6 correspond to markers adjacent to Cluster 2 on the western lobe and close to the southernmost boundary of the eastern lobe, respectively. Rainfall data are shown in terms of absolute rainfall (black line) and effective rainfall (green bars, potential evotranspiration calculated using Hydrus1D; Šimůnek et al., 2008). Cumulating the effective rainfall over the summer (red bars) and the winter (blue bars) shows a clear seasonality in the first two years, with dry summers and wet winters. It also indicates a negative water balance (i.e. potential evotranspiration larger than the amount of rainfall), which got expressed as an 18-months drought between 2010 and 2012. This seasonality is interrupted in the years 2011 and 2012 (Fig. 6). This can be attributed to a cooler and wetter than average summer in 2011 resulting in enhanced effective rainfall (absolute rainfall 10–20% higher than 30 year

average; [Belcher et al., 2014](#)) followed by a drier than average winter. The following summer of 2012 was characterised by prolonged and intense rainfall of up to 65 mm day$^{-1}$. It has been recorded as the wettest summer since 1912 ([Belcher et al., 2014](#)).

Fig. 6. Data overview showing rainfall, water level, cumulative tilt movements (i.e. absolute change in tilt meter reading), and cumulative GPS marker movements. Note the interruption in seasonality in rainfall pattern and the correlation between peaks in piezometric heads and reactivation of the landslide movements. Note that the reason for the drop of the head of the eastern piezometer below the active zone is its reinstallation to a slightly deeper level.

The seasonality of the years 2009 to 2011 can also be seen in the piezometric heads. During the winters of 2009–10 and 2010–11 the effective rainfall percolates downwards to recharge the water table resulting in elevation of piezometric heads. Conversely, in the summer, recharge diminishes and groundwater flow and discharge causes the piezometric heads to fall. The difference between summer and winter piezometric heads is about 1.8 and 1.0 m for the western and eastern lobes, respectively. Not only is the difference between summer and winter heads larger on the western lobe, it also shows more fluctuation and faster response times to rainfall events in comparison to the eastern lobe, which shows a much smoother response. This indicates that the two lobes are set within different hydrological environments. These can be characterised by (1) stronger bypass flow on the western lobe due to a higher degree of fissuring as indicated by recent infiltration experiments, and (2) the existence of sand lenses within the WMF of the western lobe providing preferential pathways for moisture drainage due to the higher permeability of those sand lenses. These two effects are less pronounced on the eastern lobe.

The surface movement indicators shown in Fig. 6 (i.e. cumulative GPS marker and tilt movement) indicate three periods of significant movement within the five year monitoring period. The first movements were recorded in October 2009, with a total of approximately 0.25 m. This movement period was brief, lasting for no longer than 2 months. After this, an 18-month period of persistent drier than average conditions caused the slope to remain in a stable condition with no movements until July 2012 when movement commenced due to the wet summer. First indication of movement during this period (Fig. 6) is given by the GPS measurements located at the front of the eastern lobe. The tilt meter of the eastern lobe shows the movements commencing in November 2012, during a period when significant movements were also recorded on the GPS markers of the eastern lobe (1.4 m between November 2012 and January 2013). This offset in the start of movement recordings may be caused by the different

sensor locations (the tilt meter is located about 20 m upslope from the marker) or by the insensitivity of the tilt meter to record pure translational movements. Movements on the western lobe commenced about 2 months after the eastern lobe, in January 2013, and lasted until April 2013. Although the tilt meter of the western lobe shows a response comparable to that on the eastern lobe, the GPS marker measurements reveal a smaller degree of movement of only about 0.25 m between November 2012 and January 2013. This period of landslide reactivation and acceleration lasted until February 2013, after which the landslide entered a period of deceleration due to a reduction of rainfall, which allowed dissipation of pore-water pressures in the slope. GPS marker measurements show that between February and October 2013 the eastern lobe moved about 0.3 m, while the western lobe reached a stable state. In the same period, the tilt meter recorded movements on both lobes. This may be explained by (1) localised surface disaggregation at or near the tilt meter, or (2) small magnitude movement that was not captured using RTK-GPS measurements (i.e. sub-mm scale). Another acceleration of movements occurred in the winter of 2013–2014, where the eastern lobe moved another 0.3 m in just one month.

The dashed horizontal lines in the piezometric head section of Fig. 6 indicate the active zone of the piezometer; the upper dashed line shows the location of the upper level of the sand pocket, which was used as reference for the piezometric head. Thus, positive heads indicate positive pore water pressure close to the slip surface. Extended periods of positive pore water pressure correlate clearly with reactivation and acceleration of the landslide on the western lobe (i.e., movement between December 2009–March 2010, and November 2012–March 2013). The piezometer on the eastern lobe shows positive pore water pressures throughout the years 2011 and 2012, with an average piezometric head of + 0.6 m above the slip surface. A global peak showing a piezometric head of + 1.5 m was recorded in November 2012 when the fastest movements commenced on this lobe. The positive piezometric head level sufficient to induce instability and movement at this location is therefore between 0.6 and 1.5 m. These movements led to a severe bending of the piezometer pipe, causing the loss of the logger. Another piezometer was installed in November 2013. This new piezometer showed positive pore water pressures immediately after its installation, correlating well with another acceleration of this lobe.

Two periods of winters 2012–13 and 2013–14 are considered in detail below. These two periods represent times at which the landslide reactivated or movement accelerated, respectively, as indicated by the GPS marker measurements. To understand the actual kinematic behaviour of the deformations, higher temporal resolution than available for

the GPS marker data is required. This is provided by the continuous or near-continuous recordings of the AEWG, SAA, and tilt meter.

4.3. Period 1 — winter 2012/2013

Fig. 7 shows period 1, which presents a time at which the landslide reactivated subsequent to more than 2 years of stability. This period, set between November 2012 and April 2013, follows a very wet summer, with rainfall exceeding 50% more than the 30-year average (Belcher et al., 2014). This intense rainfall caused the highest piezometric heads measured at the site during the 5-year monitoring period (Fig. 6). Although the high piezometric heads and thus positive pore water pressures are likely to be one of the main reasons for the reactivation and acceleration of the landslide, their highest peak has not been the ultimate trigger for the reactivation of the lobe movements. For this period the reasons for reactivation were: (1) intense rainfall leading to increased total stress due to increased moisture content; (2) loading from a rotational failure up-slope; and (3) reduction of material strength caused by elevations in pore water pressure. Fig. 7 shows that rainfall of up to 30 mm day$^{-1}$ on 25th November 2012 caused the stable slope to move. These movements have been recorded by the AEWG on the western lobe and the tilt meter on the eastern lobe. The two techniques recorded the onset of instabilities at the same time, despite being located on different lobes. At this time, no AEWG was operational on the eastern lobe. Inclinometer readings (Fig. 3) show very slow subsurface deformation from the beginning of the monitoring period in 2009 (< 50 mm year$^{-1}$) with a significant acceleration between May and October 2012 (when they eventually ceased being useable). The tilt meter and GPS markers are installed at different locations to the AEWG and inclinometer. Hence, the difference between their recordings may be an indication that the lobes move as separate blocks. Tilt meter recordings from the western and eastern lobes (and also GPS marker measurements, but with limited temporal resolution) reveal that major movements on the western lobe commenced on 16th January 2013, 51 days after movement began on the eastern lobe. At the time of slope movement initiation no intense rainfall has been recorded. Snow build-up during the several days of low temperature prior to this reactivation event resulted in 5 to 10 cm of snow cover. This snow melted as temperatures increased on 16th January 2013, which provided additional moisture to a nearly saturated subsurface (Uhlemann et al., 2014) leading to elevated pore water pressures. While smaller rainfall events (27th and 29th January with 4 and 9 mm day$^{-1}$, respectively) succeeding the snowmelt period caused further movement acceleration, a heavy rainfall event on 5th February 2013 (39 mm day$^{-1}$) did not increase the rate of

movement. This could be due to already fully saturated conditions of the lobe and thus surface runoff rather than infiltration of moisture. This heavy rainfall event was followed by a dry period leading to drainage of moisture, thus a reduction of pore water pressures, and movement decelerated. All movement indicators exhibit characteristic 'S'-shaped slope displacement-time behaviour (e.g. Allison and Brunsden, 1990, Petley et al., 2005, Smith et al., 2014); periods of acceleration followed by deceleration and stability, due to oscillations in pore water pressures in the vicinity of the shear surface. The GPS marker information did exhibit this behaviour; however, it had low temporal resolution and numerous 'S'-shaped events were not captured. The tilt meter and AEWG both captured all of the phases of reactivated movement and with a sufficient temporal resolution. This demonstrates the significance of temporal resolution in capturing landslide deformation behaviour. The time series measurements show that these periods of reactivated movement were detected at different times on the different instruments; this is because the instruments are installed at different locations on the lobes. For this five-month period of winter 2012–2013 the GPS marker measurements showed surface movements on the eastern lobe of up to 1.7 m.
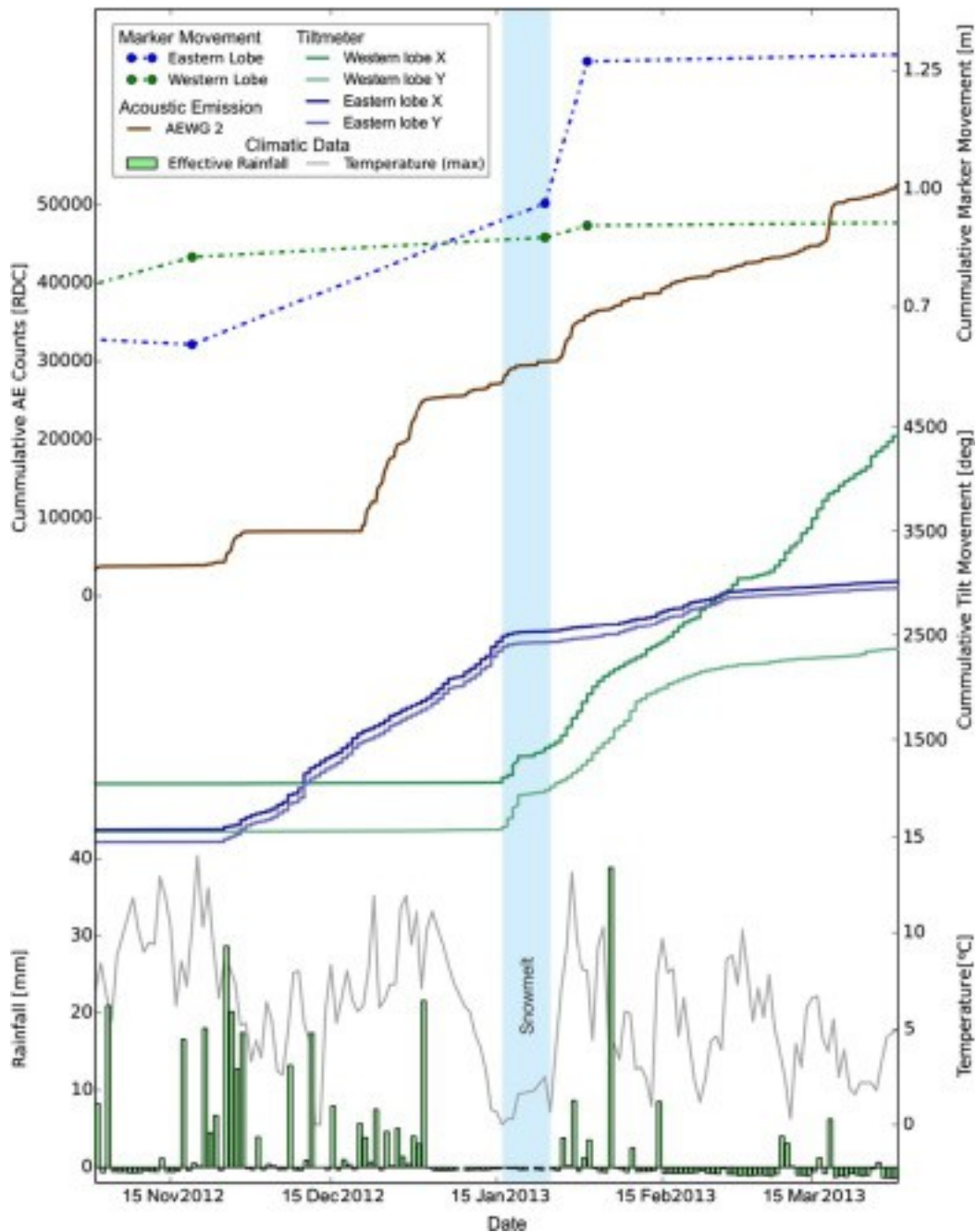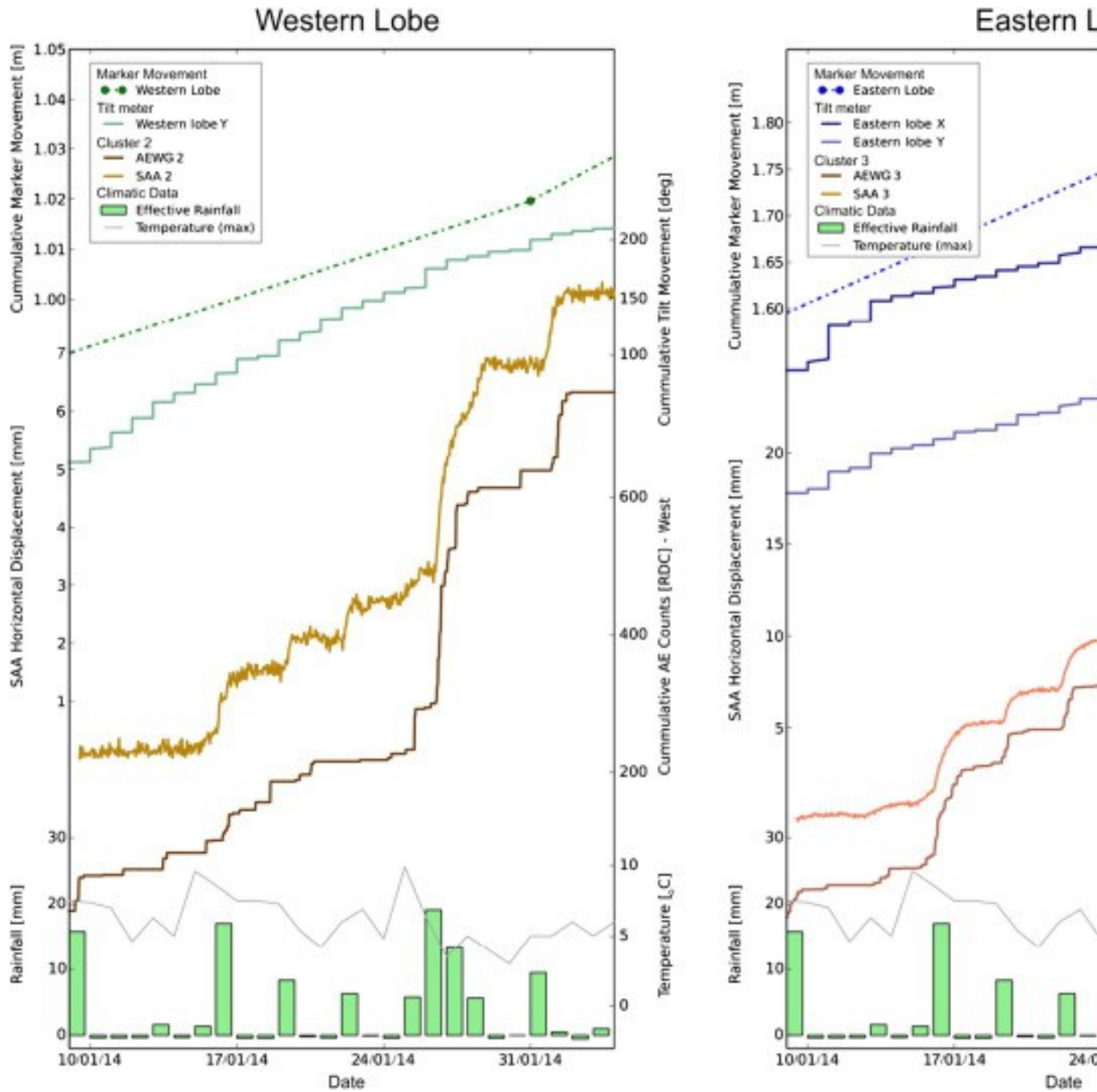
Fig. 7. Comparison of movement measurements for period 1. Shown are GPS marker, cumulative AE (RDC), and tilt meter measurements. Also shown are effective rainfall and temperature.
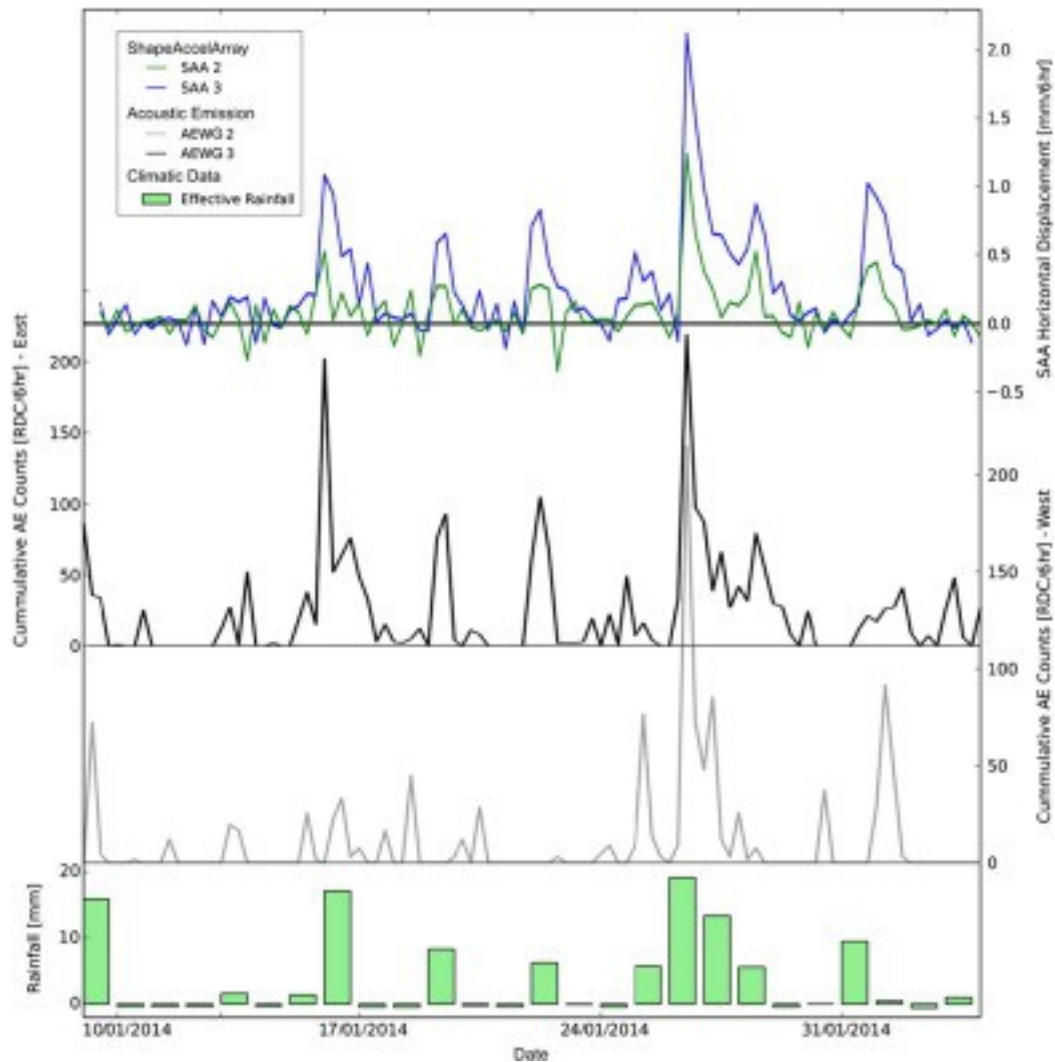
4.4. Period 2 — winter 2013/2014

The second period of landslide reactivation investigated in this paper occurred between 9th January 2014 and 4th February 2014. Period 2 has a different prehistory compared to Period 1. While Period 1 followed one of the wettest summers of recent records, Period 2 follows an average summer that led to drainage of the moisture accumulated in the slope during the winter before. Note that the weeks prior to this period were characterized by strong rainfall events, resulting in approximately 220 mm cumulative 90-day antecedent rainfall. For this period, also SAA data for the two lobes is available.

Fig. 8 shows continuous cumulative RDC- and deformation-time series measurements from active waveguides (AEWG2 and AEWG3), SAAs (SAA2 and SAA3), GPS marker, and tilt meter measurements recorded from the two lobes. The shape of the cumulative time series at both lobes are characteristic of 'S'-shaped slope movements (e.g. Allison and Brunsden, 1990, Petley et al., 2005, Smith et al., 2014). The series of slide movement events are preceded by periods of rainfall that induced transient elevations in pore water pressures along the shallow shear surface and induced movement. The slide mass accelerated towards a peak velocity and subsequently decelerated as pore-water pressures dissipated. Shear resistance was mobilised internally within the slide mass and through remoulding of the landslide toe (Dixon et al., 2014, Dixon et al., 2015). This process was repeated subsequent to each rainfall trigger as shown in Fig. 9. Fig. 9 shows the AE rates, which are the first derivative of cumulative AE and are proportional to slope velocity (Smith et al., 2014, Smith and Dixon, 2015), and SAA measured velocity at Clusters 2 and 3 for the same period of movements as in Fig. 8. Although movement appears to trigger on both lobes simultaneously, the eastern lobe clearly experienced greater magnitudes of movement as shown by GPS measurements.

1. [Download high-res image (294KB)](#)
2. [Download full-size image](#)

Fig. 8. Comparison of movement measurements for period 2. Shown are GPS marker, cumulative AE (RDC), SAA horizontal displacement measurements, and tilt meter measurements, together with effective rainfall and temperature. Note that axis for the movement measurements differ for the western and eastern lobes.

Fig. 9. First derivative of data presented in Fig. 8 showing AE rates and SAA measured velocity. Note that periods of acceleration correlate well with rainfall events. A subset of the SAA and AE measurements from the eastern lobe are also analysed in Smith et al. (2014).

Monitoring GPS markers did not provide sufficient temporal resolution to capture the 'S'-shaped phases of reactivated slope movement. The tilt meter did not capture the reactivation phases because the movements had a predominantly translational component. It is only possible to capture this slope deformation behaviour using deformation monitoring techniques that provide continuous information with high temporal resolution (e.g. AEWG and SAA), and can capture the appropriate behaviour (i.e. tilt meters are inappropriate for measuring translational movements). For a system to be capable of providing an early warning of slope instability, it must provide this level

of information, to detect accelerations of movement as early as possible and communicate them in real-time using appropriate communication systems.

The information gained from the evaluation of the movement monitoring techniques in conjunction with the accompanying rainfall and pore water pressure data led to an improved understanding of the movement pattern forming the Hollin Hill landslide in recent years. Fig. 10 shows a simplified representation of the geomorphological features and example cyclic processes underpinning the movements. Rainfall induced instabilities in the WMF of the back scarp and subsequent downslope movement of material (1 in Fig. 10) lead to an accumulation of slipped material at the WMF–SSF boundary (2). These processes, as they are rainfall dependent, show varying movement rates. Once a threshold of accumulated material and pore water pressure has been exceeded, a breakthrough occurs, transporting slipped WMF further downslope with high movement rates (3), which decrease as pore water pressures dissipate. Consequently, this material moves in a flow-like behaviour on top of the aeolian sands and the SSF, where changes in the pore water pressure levels determine the movement rates. Pore water pressures are elevated by rainfall-induced moisture input and reduced by toe-drainage through the aeolian sands and SSF. To maintain this flow-dominated process that forms the lobes of slipped WMF on top of the SSF material, input from upslope is required. The flow material is supplied episodically, following a cyclic pattern of rainfall induced deformation in the WMF, and accumulated at the WMF–SSF boundary until a stress/pore water pressure threshold is exceeded that triggers a breakthrough of a flow lobe. This cyclic behaviour is characteristic of the slopes movement during winter months when it is at its wettest and the pore water pressures in the slope are at their greatest magnitude. The slope remains predominantly stable for the remainder of the year, unless rainfall with high intensity and duration occurs.
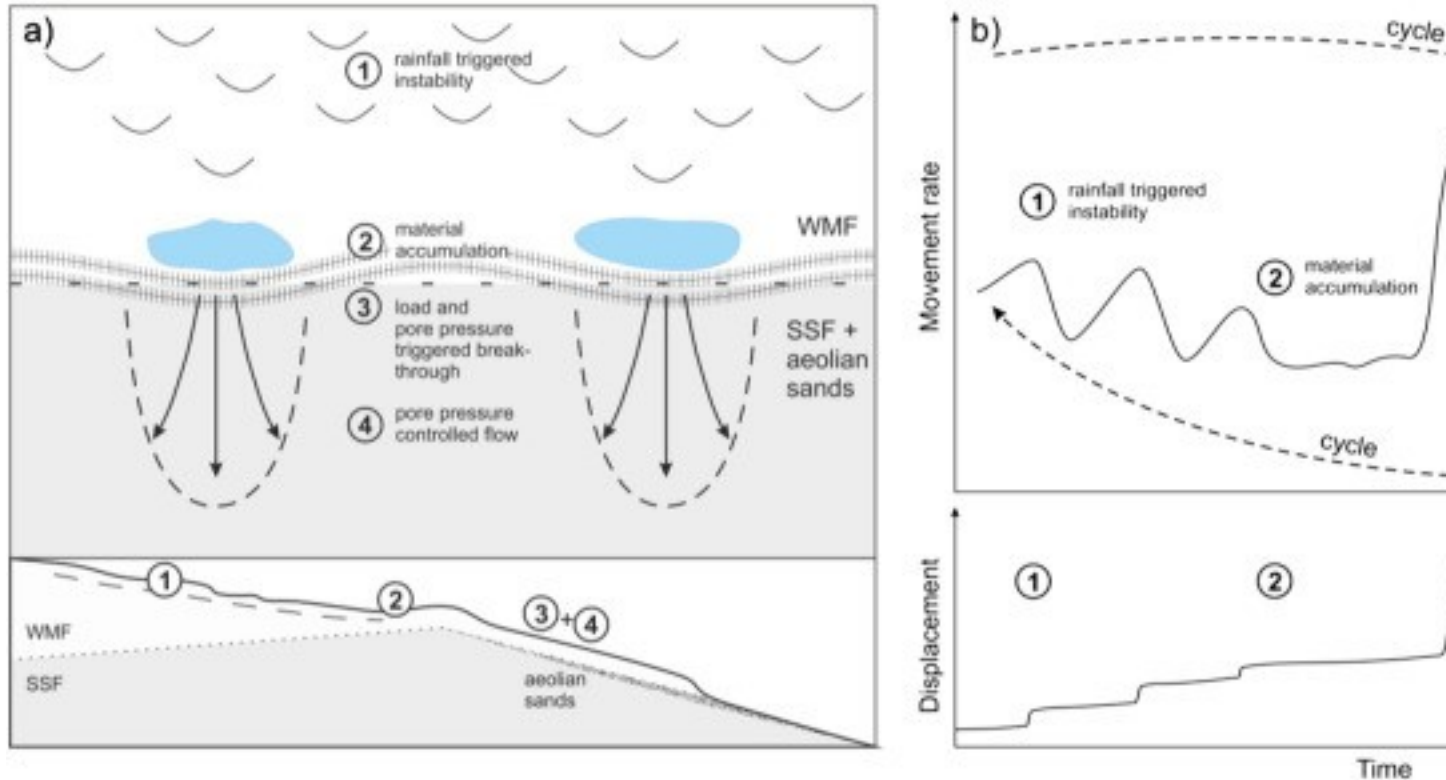
Fig. 10. Conceptual diagram of processes defining the landslide behaviour at Hollin Hill. a) Simplified plan view and cross section of Hollin Hill showing the geomorphological processes forming the landslide. b) Characteristic, cyclic movement pattern of the Hollin Hill landslide.

## 5. Discussion of technique applicability and conclusions

This paper has detailed the application of various monitoring instruments and techniques to a reactivated landslide that moves in response to rainfall-induced pore water pressure elevations. The case study has served as a comparison of the various monitoring approaches and particular attention has been given to the spatial and temporal resolution offered by the approaches.

Monitoring an array of markers installed across the slope using GPS during site visits has allowed the quantification of surface movement vectors at each marker location and therefore the identification of areas of stability/instability. This high spatial resolution information is particularly important where a large slope area is of suspected instability. The information obtained from monitoring the GPS markers can be utilised in identifying areas across the slope where further monitoring effort should be focused.

The centimetric accuracy offered by the GPS surveys is sufficient in identifying areas of relative stability across the slope and periods of movement; however, for most monitoring applications, but especially when a slope threatens infrastructure, greater accuracy in time and space is necessary. While GPS measurements are sensitive to surface deformation, acquisition of subsurface deformation information is often critical. The conventional inclinometer allows the depth to shear surface(s) to be identified. Movements over a localised depth, such as the shear surface, can be determined with an accuracy of the order of ± 0.2 mm (Mikkelsen, 2003). The inclinometer casings at Hollin Hill became unusable (i.e. would no longer allow the torpedo probe to pass the shear surface) after localised shear surface deformations of approximately 60 mm, as evidenced by the incremental readings (note Fig. 3 shows cumulative readings). Consideration should therefore be given to the life-span of such instrumentation, keeping in mind the anticipated magnitudes of movement.

Monitoring markers using GPS and inclinometer casings using torpedo probes during site visits offer low temporal resolution. This mode of monitoring informs the user whether movement occurred since the last reading but does not provide information on how and when the slope moved during this interval. It cannot provide real-time information for use in early warning. This can be overcome by using in-place probes and probe-strings installed within boreholes, providing high temporal resolution information as deformation is logged near-continuously at user-defined intervals. This study at Hollin Hill utilised SAA and AEWG to perform this function. The SAA logged deformation at 1-hour intervals using a series of MEMS installed along the depth of the borehole with accuracy of the order of ± 1.5 mm per 30 m (Abdoun et al., 2012). Additionally, AEWG monitoring provided continuous information on rates of subsurface movement, accelerations and decelerations in particular, sampled with a high temporal resolution of 30 min intervals. This high temporal resolution information provided by SAA and AEWG monitoring, was paramount in understanding the deformation behaviour of the slope in response to rainfall-induced instability. It allowed the identification of the 'S'-shaped deformation time cycles. This was not captured using the other deformation monitoring approaches. SAA and AEWG have therefore demonstrated the potential to provide early warning of movement by detecting accelerations of movement in real-time if connected to an appropriate communication system. Note that the selection of appropriate measurement intervals for these approaches is very important. An understanding of the way in which the slope will behave should inform this decision. For example, the slope at Hollin Hill is reactivated and moves in response to rainfall-induced pore water pressure elevations; these episodes of movement occur over a period of 2–3 days (Fig.

8). A monitoring frequency of the order of hours is therefore sufficient to capture this behaviour. However, when monitoring a slope that has the potential to undergo progressive first-time failure, i.e., collapse as a result of brittle strength loss (Chandler, 1984), which may experience rapid accelerations of movement over minutes or hours, a monitoring frequency of the order of minutes would be necessary to capture this behaviour and provide early warning.

Tilt meters also provide continuous information with high temporal resolution. However, as evidenced by the study at Hollin Hill, they do not successfully detect movements with predominantly translational components. This is because the instrument monitors rotation at the near-surface. Anchoring the base of the tilt meter below the slip surface offers an approach to capturing translational movements. Movement would induce bending within the tilt meter conduit, which would be measured as rotation by the tilt meter (dashed installation in Fig. 4c). Consideration should therefore be given to the use of tilt meters for slopes that are expected to have a significant rotational component of movement. For slopes with predominantly translational deformation their installation should be adapted accordingly.

Rainfall-induced elevations in pore water pressure are the main trigger for slope instability in the UK and the majority of the world. Thus, monitoring both rainfall and pore water pressures continuously with high temporal resolution provides significant opportunities in identifying critical conditions for instability. Resistance to movement is dictated primarily by the stability along shear surface(s) and therefore knowledge of pore water pressures at shear surface depth(s) is critical in understanding the stability of the slope. Piezometer tips were installed at predicted shear surface depths, which were inferred from CPT measurements at the same time as the installation of inclinometer casings. This resulted in the active zone of the piezometers being installed below the depth of the shear surfaces, as identified from subsequent inclinometer measurements. More accurate measurements of pore water pressures at the shear surface would be required for stability assessment. Therefore, it would be advisable to install piezometers at shear surfaces after their depths have been determined from inclinometer measurements. The piezometers were logged with high temporal resolution and this, in conjunction with continuous rainfall data, allowed the identification of periods of potential instability (e.g. Fig. 6 and Section 4.2). This level of information can be taken to develop rainfall intensity–duration relationships (e.g. Caine, 1980) and critical pore water pressures to allow prediction/forecasting of instability for the slope.

Stability assessment of slopes requires information that inclinometers and standpipes can provide such as shear surface depths and ground water levels. However, in order to

inform ongoing risk assessments and numerical modelling of slope stability, and to provide early warning of instability, greater knowledge of the slopes behaviour must be acquired. This can be achieved by using combinations of instruments and techniques. This combination should cover instrumentation that provides high temporal and spatial resolutions, both at the measurement and slope scale. While high spatial resolution at the slope scale usually omits high spatial resolution at the measurement scale and high temporal resolution, it provides the necessary information for targeted installation of sensors that can subsequently provide the necessary high resolution data at those scales. For high temporal resolution data that inform early warning systems, a telemetric link between the field site and a database is required. Methods to deliver those data in real-time to web-platforms informing not only engineers and scientists but the wider public about potential hazards are becoming more frequently implemented in recent years (Reid et al., 2012, Huang et al., 2015), but still require more research on how to manage the available data and present it in an informative fashion.

Although it is a significant constraint on the majority of projects, the cost of monitoring and of each instrument and technique has not been discussed in this paper. However, with rapidly developing technologies and greater awareness of the value that monitoring can bring to projects, such instruments and techniques are expected to become more widely used in the future. This case study provides an example of various techniques and instruments applied to a landslide over a 5-year period. It has demonstrated the level of information attainable from the combination of instruments and techniques, in order to capture both spatial and temporal behaviour. It showed that only a well-balanced choice of monitoring devices covering all scales of spatial and temporal resolutions delivers information that can be used to understand triggering mechanisms and deformation behaviour of a slope in great detail.

## Acknowledgements

# References

Abdoun et al., 2012

T. Abdoun, V. Bennett, T. Desrosiers, J. Simm, M. Barendse**Asset management and safety assessment of levees and earthen dams through comprehensive real-time field monitoring**

Geotech. Geol. Eng., 31 (2012), pp. 833-843, 10.1007/s10706-012-9569-3

View Record in Scopus

Allison and Brunsden, 1990

R.J. Allison, D. Brunsden**Some mudslide movement patterns**

Earth Surf. Process. Landf., 15 (1990), pp. 297-311, 10.1002/esp.3290150402

CrossRefView Record in Scopus

Angeli et al., 2000

M.-G. Angeli, A. Pasuto, S. Silvano**A critical review of landslide monitoring experiences**

Eng. Geol., 55 (2000), pp. 133-147, 10.1016/S0013-7952(99)00122-2

ArticleDownload PDFView Record in Scopus

Ballantyne and Harris, 1994

C.K. Ballantyne, C. Harris**The Periglaciation of Great Britain**

Cambridge University Press, Cambridge (1994)

Bateman, 1995

M.D. Bateman**Thermoluminescence dating of the British coversand deposits**

Quat. Sci. Rev., 14 (1995), pp. 791-798, 10.1016/0277-3791(95)00053-4

ArticleDownload PDFView Record in Scopus

Belcher et al., 2014

S. Belcher, J. Slingo, R. McCarthy, C. Burton, R. Betts, S. Brown, R. Clark, R. Kahana, E. Kendon, J. Knight, M. McCarthy, D. McNeall, D. Sexton, P. Stott**Too Hot, Too Cold, Too Wet, Too Dry : Drivers and Impacts of Seasonal Weather in the UK**

MetOffice, Exeter (2014)

Brückl et al., 2013

E. Brückl, F.K. Brunner, E. Lang, S. Mertl, M. Müller, U. Stary**The Gradenbach Observatory-monitoring deep-seated gravitational slope deformation by geodetic, hydrological, and seismological methods**

Landslides, 10 (2013), pp. 815-829, 10.1007/s10346-013-0417-1

CrossRefView Record in Scopus

Buchli et al., 2012

B. Buchli, F. Sutton, J. Beutel**GPS-equipped wireless sensor network node for high-accuracy positioning applications**

P. GianPietro, W. Heinzelman (Eds.), Wireless Sensor Networks, Springer, Berlin Heidelberg (2012), pp. 179-195, 10.1007/978-3-642-28169-3_12

CrossRefView Record in Scopus

Buchli et al., 2013

T. Buchli, K. Merz, X. Zhou, W. Kinzelbach, S.M. Springman**Characterization and monitoring of the Furggwanghorn Rock Glacier, Turtmann Valley, Switzerland: results from 2010 to 2012**

Vadose Zone J., 12 (2013), pp. 1-15, 10.2136/vzj2012.0067

Caine, 1980

N. Caine**The rainfall intensity: duration control of shallow landslides and debris flows**

Geogr. Ann. Ser. A, Phys. Geogr., 62 (1980), pp. 23-27, 10.2307/520449

CrossRefView Record in Scopus

Catt, 1977

J.A. Catt**Loess and coversands**

F.W. Shotton (Ed.), British Quaternary Studies — Recent Advances, Clarendon Press, Oxford (1977), pp. 221-230

View Record in Scopus

Chambers et al., 2011

J.E. Chambers, P.B. Wilkinson, O. Kuras, J.R. Ford, D.A. Gunn, P.I.Meldrum, C.V.L. Pennington, A.L. Weller, P.R.N. Hobbs, R.D. Ogilvy**Three-dimensional geophysical anatomy of an active landslide in Lias Group mudrocks, Cleveland Basin, UK**

Geomorphology, 125 (2011), pp. 472-484, 10.1016/j.geomorph.2010.09.017

ArticleDownload PDFView Record in Scopus

Chandler, 1984

R. Chandler**Recent European experience of landslides in over-consolidated clays and soft rocks**

4th International Symposium on Landslide. Toronto (1984), pp. 61-80

View Record in Scopus

Corsinietal

A. Corsini, A. Pasuto, M. Soldati, A. Zannoni**Field monitoring of the Corvara landslide (Dolomites, Italy) and its relevance for hazard assessment**
Geomorphology, 66 (2005), pp. 149-165, [10.1016/j.geomorph.2004.09.012](#)
[ArticleDownload PDFView Record in Scopus](#)

D.M. Cruden, D.J. Varnes**Landslide types and processes. In: Turn, A.K., Schuster, R.L. (Eds.) Landslides Investig. Mitigation**
Spec. Rep., 247 (1996), pp. 36-75
[View Record in Scopus](#)

Defra**UK Climate Change Risk Assessment: Evidence Report (No. GA0204)**
Defra, London (2012)

T.A. Dijkstra, N. Dixon**Climate change and slope stability in the UK: challenges and approaches**
Q. J. Eng. Geol. Hydrogeol., 43 (2010), pp. 371-385, [10.1144/1470-9236/09-036](#)
[CrossRefView Record in Scopus](#)

T. Dijkstra, N. Dixon, C. Crosby, M. Frost, D. Gunn, P. Fleming, J. Wilks**Forecasting infrastructure resilience to climate change**
Proc. Inst. Civ. Eng., 167 (2014), pp. 269-280
[CrossRefView Record in Scopus](#)

Dixon, N., Spriggs, M., 2011. Apparatus and method for monitoring soil slope displacement rate. UK Patent 2467419A.

N. Dixon, M.P. Spriggs, A. Smith, P. Meldrum, E. Haslam**Quantification of reactivated landslide behaviour using acoustic emission monitoring**
Landslides (2014), [10.1007/s10346-014-0491-z](#)

Dixon et al., 200?

N. Dixon, R. Hill, J. Kavanagh**Acoustic emission monitoring of slope instability: development of an active waveguide system**

Proc. ICE Geotech. Eng. (2003), [10.1680/geng.2003.156.2.83](10.1680/geng.2003.156.2.83)

Dixon et al., 201(

N. Dixon, M. Spriggs, P. Meldrum, R. Ogilvy**Development of a low cost acoustic emission early warning system for slope instability**

A.L. Williams (Ed.), Geologically Active: Proceedings of the 11th IAEG Congress, CRC Press, Auckland, New Zealand (2010), pp. 1803-1810

[View Record in Scopus](View Record in Scopus)

Dixon et al., 2015

N. Dixon, A. Smith, M. Spriggs, A. Ridley, P. Meldrum, E. Haslam**Stability monitoring of a rail slope using acoustic emission. Proc. Inst. Civ. Eng. — Geotech**

Engl. J., 168 (2015), pp. 373-384, [10.1680/jgeen.14.00152](10.1680/jgeen.14.00152)

[CrossRef](CrossRef)[View Record in Scopus](View Record in Scopus)

Dunnicliff, 1988

J. Dunnicliff**Geotechnical Instrumentation for Monitoring Field Performance**

John Wiley & Sons, New York (1988)

Foster et al., 201

C. Foster, C.V.L. Pennington, M.G. Culshaw, K. Lawrie**The national landslide database of Great Britain: development, evolution and applications**

Environ. Earth Sci., 66 (2011), pp. 941-953, [10.1007/s12665-011-1304-5](10.1007/s12665-011-1304-5)

Füssel et al., 201

H.-M. Füssel, A. Jol, M. Hildén**Climate change, impacts and vulnerability in Europe 2012 — An Indicator-based Report (No. 12/2012)**

EEA — European Environment Agency, Luxembourg (2012), [10.2800/66071](10.2800/66071)

García et al., 201

a. García, A. Hördt, M. Fabian**Landslide monitoring with high resolution tilt measurements at the Dollendorfer Hardt landslide, Germany**

Geomorphology, 120 (2010), pp. 16-25, [10.1016/j.geomorph.2009.09.011](10.1016/j.geomorph.2009.09.011)

[Article](Article)[Download PDF](Download PDF)[View Record in Scopus](View Record in Scopus)

Gaunt et al., 198

G.D. Gaunt, H.C. Ivimey-Cook, I.E. Penn, B.M. Cox**Mesozoic Rocks Proved by IGS Boreholes in the Humber and Acklam Areas**

Institute of Geological Studies, Nottingham (1980)

Glendinning et a

S. Glendinning, J. Hall, L. Manning**Asset-management strategies for infrastructure embankments**

Proc. ICE Eng. Sustain. (2009), [10.1680/ensu.2009.162.2.111](10.1680/ensu.2009.162.2.111)

Glendinning et a

S. Glendinning, P.R. Helm, M. Rouainia, R.A. Stirling, J.D. Asquith, P.R.N. Hughes, D.G. Toll, D. Clarke, W. Powrie, J. Smethurst, D. Hughes, R. Harley, R.Karim, N. Dixon, C. Crosby, J. Chambers, T.A. Dijkstra, D. Gunn, K. Briggs, D. Muddle**Research-informed Design, Management and Maintenance of Infrastructure Slopes: Development of a Multi-Scalar Approach**
IOP Conference Series, Earth and Environmental Science (EES) (2015)

Gunn et al., 201

D.A. Gunn, J.E. Chambers, P.R.N. Hobbs, J.R. Ford, P.B. Wilkinson, G.O.Jenkins, A. Merritt**Rapid observations to guide the design of systems for long-term monitoring of a complex landslide in the Upper Lias clays of North Yorkshire, UK**
Q. J. Eng. Geol. Hydrogeol., 46 (2013), pp. 323-336, [10.1144/qjegh2011-028](https://doi.org/10.1144/qjegh2011-028)
CrossRefView Record in Scopus

Highland and Bo

L. Highland, P. Bobrowsky**The Landslide Handbook: A Guide to Understanding Landslides**
U.S. Geolo. ed, Reston, Virginia (2008)

Huang et al., 201

H. Huang, W. Yi, Q. Yi, S. Lu**Real-time monitoring and data analysis of an active landslide in the Three Gorges Reservoir**
G. Lollino, D. Giordan, G.B. Crosta, J. Corominas, R. Azzam, J. Wasowski, N. Sciarra(Eds.), Engineering Geology for Society and Territory — Volume 2 SE — 253, Springer International Publishing (2015), pp. 1433-1436, [10.1007/978–3-319-09057-3_253](https://doi.org/10.1007/978-3-319-09057-3_253)
CrossRefView Record in Scopus

Kuras et al., 200

O. Kuras, J.D. Pritchard, P.I. Meldrum, J.E. Chambers, P.B. Wilkinson, R.D.Ogilvy, G.P. Wealthall**Monitoring hydraulic processes with automated time-lapse electrical resistivity tomography (ALERT)**
C. R. Geosci., 341 (2009), pp. 868-885, [10.1016/j.crte.2009.07.010](https://doi.org/10.1016/j.crte.2009.07.010)
ArticleDownload PDFView Record in Scopus

Machan and Bec

G. Machan, D. Beckstrand**Practical considerations for landslide instrumentation**
E. Eberhardt, C. Froese, K. Turner, S. Leroueil (Eds.), Landslides and Engineered Slopes: Protecting Society through Improved Understanding (2012), pp. 1229-1234
View Record in Scopus

Malet et al., 200

J.-P. Malet, O. Maquaire, E. Calais**The use of Global Positioning System techniques for the continuous monitoring of landslides: application to the Super-Sauze earthflow (Alpes-de-Haute-Provence, France)**
Geomorphology, 43 (2002), pp. 33-54, [10.1016/S0169-555X(01)00098-8](https://doi.org/10.1016/S0169-555X(01)00098-8)
ArticleDownload PDFView Record in Scopus

Merritt et al., 201

A.J. Merritt, J.E. Chambers, W. Murphy, P.B. Wilkinson, L.J. West, D.A. Gunn, P.I. Meldrum, M. Kirkham, N. Dixon**3D ground model development for an active landslide in Lias mudrocks using geophysical, remote sensing and geotechnical methods**
Landslides, 11 (2013), pp. 537-550, [10.1007/s10346-013-0409-1](10.1007/s10346-013-0409-1)

Mikkelsen, 2003

P. Mikkelsen**Advances in inclinometer data analysis**
F. Myrvoll (Ed.), 6th International Symposium on Field Measurements in Geomechanics, Oslo, Norway (2003), pp. 1-13
[View Record in Scopus](View Record in Scopus)

Pennington et al

C. Pennington, K. Freeborough, C. Dashwood, T. Dijkstra, K. Lawrie**The national landslide database of Great Britain: acquisition, communication and the role of social media**
Geomorphology, 249 (2015), pp. 44-51, [10.1016/j.geomorph.2015.03.013](10.1016/j.geomorph.2015.03.013)
[ArticleDownload PDFView Record in Scopus](ArticleDownload PDFView Record in Scopus)

Petley, 2012

D. Petley**Global patterns of loss of life from landslides**
Geology, 40 (2012), pp. 927-930, [10.1130/G33217.1](10.1130/G33217.1)
[CrossRefView Record in Scopus](CrossRefView Record in Scopus)

Petley et al., 200

D.N. Petley, F. Mantovani, M.H. Bulmer, A. Zannoni**The use of surface monitoring data for the interpretation of landslide movement patterns**
Geomorphology, 66 (2005), pp. 133-147, [10.1016/j.geomorph.2004.09.011](10.1016/j.geomorph.2004.09.011)
[ArticleDownload PDFView Record in Scopus](ArticleDownload PDFView Record in Scopus)

Powell, 1984

J.H. Powell**Lithostratigraphical nomenclature of the Lias Group in the Yorkshire Basin**
Proc. Yorks. Geol. Soc., 45 (1984), pp. 51-57, [10.1144/pygs.45.1-2.51](10.1144/pygs.45.1-2.51)
[CrossRefView Record in Scopus](CrossRefView Record in Scopus)

Powell, 2010

J.H. Powell**Jurassic sedimentation in the Cleveland Basin: a review**
Proc. Yorks. Geol. Soc., 58 (2010), pp. 21-72, [10.1144/pygs.58.1.278](10.1144/pygs.58.1.278)
[CrossRefView Record in Scopus](CrossRefView Record in Scopus)

Reid et al., 2012

M.E. Reid, R.G. Lahusen, R.L. Baum, J.W. Kean, W.H. Schulz, L.M. Highland**Real-time monitoring of landslides**
U.S. Geological Survey Fact Sheet 2012–3008 (2012)
(4 pp.)

Simeoni and Mo

L. Simeoni, L. Mongiovì**Inclinometer monitoring of the Castelrotto landslide in Italy**

J. Geotech. Geoenviron. Eng., 133 (2007), pp. 653-666, 10.1061/(ASCE)1090-0241(2007)133:6(653)

CrossRefView Record in Scopus

Šimůnek et al., 2

J. Šimůnek, M.T. van Genuchten, M. Šejna**Development and applications of the HYDRUS and STANMOD software packages and related codes**

Vadose Zone J., 7 (2008), pp. 587-600, 10.2136/vzj2007.0077

CrossRefView Record in Scopus

Smith and Dixon, 2015

A. Smith, N. Dixon**Quantification of landslide velocity from active waveguide–generated acoustic emission**

Can. Geotech. J., 52 (2015), pp. 413-425, 10.1139/cgj-2014-0226

CrossRefView Record in Scopus

Smith et al., 2014

A. Smith, N. Dixon, P. Meldrum, E. Haslam, J. Chambers**Acoustic emission monitoring of a soil slope: comparisons with continuous deformation measurements**

Geotech. Lett., 4 (2014), pp. 255-261, 10.1680/geolett.14.00053

CrossRefView Record in Scopus

Springman et al., 2013

S.M. Springman, P. Kienzler, S. Friedel**A long-term field study for the investigation of rainfall-induced landslides**

Géotechnique, 63 (2013), pp. 1177-1193, 10.1680/geot.11.P.142

CrossRefView Record in Scopus

Uhlemann et al., 2014

S. Uhlemann, J. Chambers, A. Merritt, P. Wilkinson, P. Meldrum, D. Gunn, H. Maurer, N. Dixon**Integrated interpretation of geophysical, geotechnical, and environmental monitoring data to define precursors for landslide activation**

AGU Fall Meeting. San Francisco, USA (2014)

Uhlemann et al., 2015

S. Uhlemann, P. Wilkinson, J. Chambers, H. Maurer, A. Merritt, D. Gunn, P. Meldrum**Interpolation of landslide movements to improve the accuracy of 4D geoelectrical monitoring**

J. Appl. Geophys., 121 (2015), pp. 93-105, 10.1016/j.jappgeo.2015.07.003

ArticleDownload PDFView Record in Scopus

Wan and Standing, 2014

M.S.P. Wan, J.R. Standing**Lessons learnt from installation of field instrumentation**

Proc. ICE Geotech. Eng., 167 (2014), pp. 491-506

CrossRefView Record in Scopus

Wilkinson et al., 2010

P.B. Wilkinson, J.E. Chambers, P.I. Meldrum, D.A. Gunn, R.D. Ogilvy, O.Kuras**Predicting the movements of permanently installed electrodes on an active landslide using time-lapse geoelectrical resistivity data only**

Geophys. J. Int., 183 (2010), pp. 543-556

[CrossRef](#)[View Record in Scopus](#)

[Wilkinson et al., 2015](#)

P.B. Wilkinson, S. Uhlemann, J.E. Chambers, P.I. Meldrum, M.H. Loke**Development and testing of displacement inversion to track electrode movements on 3-D electrical resistivity tomography monitoring grids**

Geophys. J. Int., 200 (2015), pp. 1566-1581, [10.1093/gji/ggu483](#)

[CrossRef](#)[View Record in Scopus](#)